

Light that appears to come from a source that does not existItamar Stern,¹ Yakov Bloch,² Einav Grynszpan,¹ Merav Kahn¹ ,¹ Yakir Aharonov,^{3,4,5}
Justin Dressel,^{4,5} Eliahu Cohen⁶ , and John C. Howell^{4,5,1} ¹*Racah Institute of Physics, The Hebrew University of Jerusalem, Jerusalem 91904, Israel*²*Department of Physics, Bar-Ilan University, Ramat Gan 5290002, Israel*³*School of Physics and Astronomy, Tel Aviv University, Tel Aviv 6997801, Israel*⁴*Institute for Quantum Studies, Chapman University, 1 University Drive, Orange, California 92866, USA*⁵*Schmid College of Science and Technology, Chapman University, 1 University Drive, Orange, California 92866, USA*⁶*Faculty of Engineering and the Institute of Nanotechnology and Advanced Materials, Bar-Ilan University, Ramat Gan 5290002, Israel*

(Received 10 October 2023; accepted 11 December 2023; published 9 January 2024)

Superoscillatory, band-limited functions oscillate faster than their fastest Fourier component. Superoscillations have been intensively explored recently as they give rise to many out-of-the-spectrum phenomena entailing both fundamental and applied significance. We experimentally demonstrate a form of superoscillations which is manifested by light apparently coming from a source located far away from the actual one. These superoscillations are sensed through sharp transverse shifts in the local wave vector at the minima of a pinhole diffraction pattern. We call this phenomenon “optical ventriloquism.”

DOI: [10.1103/PhysRevA.109.012206](https://doi.org/10.1103/PhysRevA.109.012206)**I. INTRODUCTION**

As anticipated in Ref. [1] and developed in Refs. [2,3], superoscillations give rise to nonintuitive and mathematically rich phenomena. Superoscillations of a band-limited signal produce spatially local regions that exhibit frequencies exceeding the highest Fourier component of the signal [3–8]. Superoscillations are general wave phenomena appearing in both classical and quantum contexts. Classically, they have been studied in a wide variety of systems including optical [9,10], acoustic [9,11,12], and radio-frequency systems [13]. Quantum mechanically, they have also been intensively studied [2,4,14,15]. Notably, such superoscillatory behavior has been shown in Refs. [14,16] to be tightly connected to the appearance of anomalous weak values [17–20], which are conditioned values of quantum observables that exceed their spectral bounds.

A vivid connection between superoscillations and weak values was recently demonstrated theoretically in Ref. [21], which showed that by means of pre- and postselection it is possible to make the spontaneous emission from a superposed atom appear as if it had come from a different location than the atom itself. In some respects, this gedanken experiment, which relies on anomalous weak values [17–20], is a spatial dual to traditional frequency-focused superoscillations. That is, wave interference within a narrow band of wave vectors yields an apparent spatial location outside the region expected from the total signal. A similar observation that anomalous spatial shifts can occur in reflected optical beams was thoroughly explored in Refs. [22–26], which very productively highlighted the utility and versatility of the weak value formalism in analyzing such counterintuitive effects even outside quantum theory.

In this paper, we theoretically analyze and experimentally demonstrate another counterintuitive manifestation of

superoscillations. We show that Alice can prepare and broadcast a (preselected) optical signal such that when Bob later intercepts this signal at a particular (postselected) position, the source of that signal will appear at Bob’s detector to come from a different location than Alice’s. We call this phenomenon “optical ventriloquism” as the light seems to be emitted from a nonexistent and spatially shifted source, as shown in Fig. 1. Our proof-of-principle experiment consists of a purely classical setup that allows the observation of this phenomenon. The main result presented in this work is a general wave phenomenon, closely related to the singularities of light as extensively discussed by Berry [27].

The apparent source will shift if the local wave vector seen at the detector no longer points radially from the source. For this to happen, the local optimal momentum streamlines must deviate from the ray-tracing predicted by geometric optics. Counterintuitively, optical streamlines can bend even without an anisotropic medium in between the source and detector if the field amplitude varies locally, as pointed out by Berry [28,29]. Such “self-bendings” of local wave-vector streamlines were experimentally confirmed by Kocsis *et al.* in a single-photon double-slit experiment [30], and later identified as the orbital part of the electromagnetic Poynting vector by Bliokh *et al.* [31]. In this work, we point out the possible utility of such a self-bending effect to spoof the location of a source at a specific location where a detector is anticipated to reside.

The rest of the paper is organized as follows. In the next section we describe the theory underlying the experiment. We then describe the experimental setup and analyze its results, showing the optical ventriloquism effect. We conclude with a short discussion regarding the achievements of this work as well as some prospective research directions.

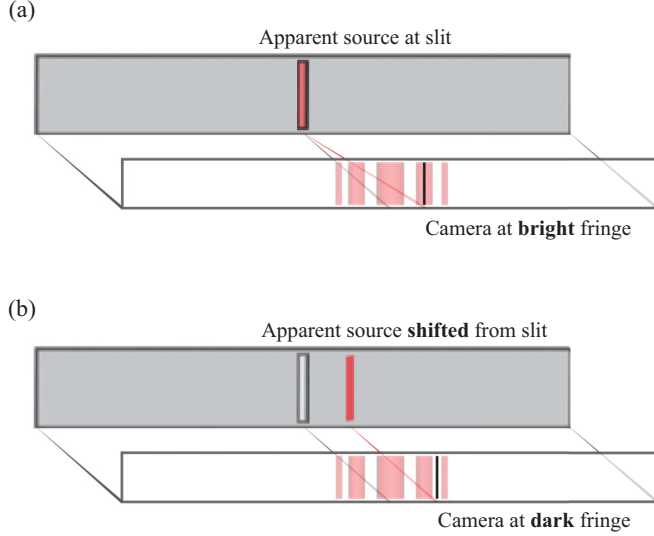


FIG. 1. Diagrammatic sketch of optical ventriloquism. The source and detection planes are parallel to each other. (a) Placing the measuring slit and camera in the middle of a bright fringe in the measurement plane will show an apparent source localized at the slit, as expected. (b) In contrast, placing the slit and camera within a dark fringe apparently shows a horizontally shifted source, making it seem as if the light came from a location where there was no actual source.

II. THEORY

Light rays can bend locally in counterintuitive ways near interference minima. To understand why, consider a monochromatic scalar wave $\Psi(\vec{r}, t) = \exp(-i\omega t) \psi(\vec{r})$ of frequency ω in a medium with an index of refraction n , with a spatial amplitude $\psi(\vec{r})$ that we write in both Cartesian and polar forms,

$$\psi(\vec{r}) = a(\vec{r}) + ib(\vec{r}) = A(\vec{r}) \exp[ik_0\phi(\vec{r})]. \quad (1)$$

Here, the free-space wave number k_0 is related to the frequency ω by the speed of light in vacuum $c = \omega/k_0$, while the wave number in the medium is nk_0 . By construction of the polar form, the *local* wave vector $\vec{k}(\vec{r})$ seen at a particular point \vec{r} is determined by the gradient of the phase [28]:

$$\vec{k}(\vec{r}) = k_0 \nabla \phi = \frac{1}{A^2} (-b \nabla a + a \nabla b) = \text{Re} \frac{\langle \vec{r} | \hat{k} | \psi \rangle}{\langle \vec{r} | \psi \rangle}. \quad (2)$$

The last equality uses the identification $\psi(\vec{r}) \equiv \langle \vec{r} | \psi \rangle$ to express the local wave vector as a *weak value* [17] of the wave-vector operator \hat{k} , postselected on a particular spatial location $\langle \vec{r} |$, with the wave-vector operator defined in an analogous way to the quantum momentum operator $\langle \vec{r} | \hat{k} | \psi \rangle = -i \nabla \langle \vec{r} | \psi \rangle$.

A superposition of waves is *superoscillatory* at location \vec{r} if its local wave number $|\vec{k}(\vec{r})|$ lies outside the Fourier spectra of the waves composing the superposition [32]. That is, the local weak value of the wave-vector operator \hat{k} has a magnitude outside the bounds of its spectrum in the initial superposition state $|\psi\rangle$, making it an anomalous weak value. For a monochromatic light beam diffracting through a slit, for example, all radially propagating Huygens components of

the outgoing superposition have the same wave number nk_0 , so a local wave vector $\vec{k}(\vec{r})$ will be outside the spectrum if $|\vec{k}(\vec{r})| \neq nk_0$. As shown below, regions of such anomalous local wave vectors will naturally appear where the amplitude $A(\vec{r})$ changes.

To see how such anomalous behavior occurs, we examine the structure of the wave equation. The wave equation satisfied by $\Psi(\vec{r}, t)$ reduces to the Helmholtz equation for the spatial amplitude $\psi(\vec{r})$, $\nabla^2 \psi + (nk_0)^2 \psi = 0$, which can be written as [33]

$$k_0^2 (n^2 - |\nabla \phi|^2) A + \nabla^2 A - ik_0 (2 \nabla \phi \cdot \nabla A + A \nabla^2 \phi) = 0. \quad (3)$$

This complex equation splits into two coupled real *eikonal equations* that constrain the local wave vector,

$$|\vec{k}|^2 = (n\omega/c)^2 + (\nabla^2 A)/A, \quad \nabla \cdot \vec{k} = 2 \vec{k}_A \cdot \vec{k}, \quad (4)$$

where $\vec{k}_A(\vec{r}) = \nabla \ln A^{-1} = \text{Im} \langle \vec{r} | \hat{k} | \psi \rangle / \langle \vec{r} | \psi \rangle$ is the imaginary part of the same wave-vector weak value in Eq. (2).

The standard geometrical optics limit assumes that the wave intensity A^2 is slowly varying, $(n\omega/c)^2 \gg |(\nabla^2 A)/A|$, such that the eikonal Eqs. (4) approximate $|\nabla \phi|^2 \approx n^2$ and $\nabla^2 \phi \approx 0$. The solutions of these simplified eikonal equations correspond to smooth particlelike streamlines that are sufficient for most ray-tracing applications [34]. Notably, amplitude variations outside this ray-tracing regime make the second term in Eq. (2) relevant and produce anomalous wave vectors $|\vec{k}| \neq nk_0$. When $|\vec{k}| > nk_0$ the local wave vector becomes *superoscillating* [32]. We now demonstrate this effect experimentally by examining the structure of local wave vectors near a single-slit interference minimum.

III. EXPERIMENT

We performed an experiment to demonstrate the self-bending of light. As discussed earlier, these self-bending effects only occur in regions of superoscillatory behavior. We performed a postselection on an interference pattern in the Fresnel region near the interference minima (i.e., A small).

Our experimental scheme is depicted in Fig. 2. A 633-nm HeNe laser beam propagates through a circular pinhole with the diameter of 200 μm . A second pinhole of 10 μm diameter postselects a small area of the first pinhole interference pattern. It is important to note, the dimensions of the second pinhole were chosen such that its transverse dimension is much smaller than the width of the interference fringe. This ensures that the postselected region was small enough to include only a region of similar k vectors.

After the second pinhole, a scientific complementary metal-oxide-semiconductor (sCMOS) camera is used for image acquisition. The detection scheme includes the second pinhole mounted on a stackable lens mount and screwed in place of the camera cap ensuring the pinhole was centered and fixed in place relative to the camera detector. The camera was set on a precision motorized track to horizontally scan the original first pinhole interference pattern. Relative to the camera detector, the first pinhole is set a distance of 7.8 cm and the second at 1.1 cm.

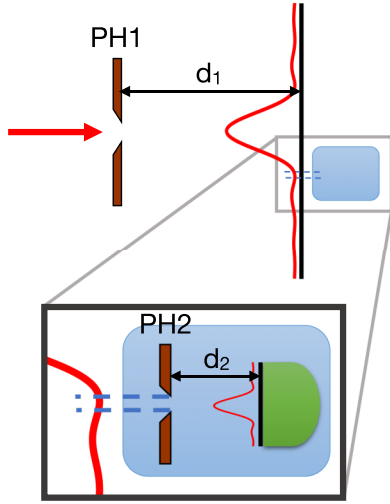


FIG. 2. Experimental setup. A 633-nm HeNe laser beam diffracts through a pinhole (PH1) with a 200- μm aperture to create an interference pattern on an image plane $d_1 = 6.7$ cm behind the pinhole. A motorized stage (inset in blue) scans along this image plane, containing a second movable pinhole (PH2) with a 10- μm aperture and an sCMOS camera placed at a distance of $d_2 = 1.1$ cm behind the second pinhole. The transverse shift x in the mean intensity recorded by the camera relative to the second pinhole indicates the angle of transverse local wave vector at the image plane according to $x/d_2 = k_x/k_z = \tan[\arg(\vec{k})]$.

The detection scheme was placed before the Fraunhofer regime. Fraunhofer diffraction is defined by $\frac{ka^2}{2z} \ll 1$ for a pinhole of diameter a observed at a distance z . Our parameters give $\frac{ka^2}{2z} \approx 0.5$, situating the experiment in the Fresnel approximation region and providing imperfect interference at the minima, allowing for a small amount of light to reach the camera detector. Further, the closer the detector is to the source, the stronger are the spatial-amplitude variations, resulting in a large $\nabla^2 A$ term.

Data for this experiment were obtained by running the horizontal scan twice. For the first run, the camera was set to a constant exposure to obtain the power distribution of a horizontal cut along the single pinhole diffraction pattern. In postprocessing, the integrated flux of each frame was used to obtain a value for the relative intensity at each camera position. As expected, this simply reconstructs the results of the familiar pinhole experiment identical to the black curve in Fig. 3.

For the second run, the camera was set to automatic exposure, adapting to the varying intensity while scanning across the fringes. This allowed to measure a sufficient signal to see the deflection of the beam in the intensity minima as shown by the blue curve in Fig. 3. For a video of the scan, see Ref. [35]. The transverse shifts x of the centroid of the optical pattern on the camera relative to the pinhole were used to measure the change in direction of the local wave vector \vec{k} at the second pinhole (PH2) according to

$$\tan[\arg(\vec{k})] = \frac{x}{d_2} = \frac{k_x}{k_z}. \quad (5)$$

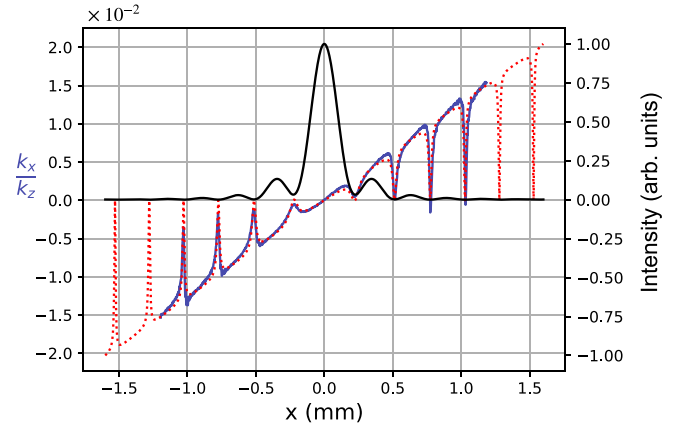


FIG. 3. Superoscillations from a pinhole diffraction pattern manifest as sharp transverse shifts of the k vector at minima of the pattern: In solid blue, the experimental results. In the dotted red, theoretical results obtained from simulation. In black, extracted from the same simulation, a horizontal cut of the diffraction pattern.

These measured position-dependent transverse shifts are shown in Fig. 3 (blue solid curve) and compared to the shifts expected from the analysis in the next section (red dashed curve).

IV. ANALYSIS

We predict the wave propagation pattern from a pinhole at a distant plane using the Fresnel approximation to simulate the k -vector behavior. The simulation calculates the field at distance z as $U(x, y, z)$, given the initial field $U(x, y, 0)$ at the plane of the first pinhole using the following Fresnel integral,

$$U(x, y, z) = \frac{e^{ikz}}{i\lambda z} \iint_{-\infty}^{+\infty} U(x', y', 0) e^{i\frac{\pi}{\lambda z}[(x-x')^2 + (y-y')^2]} dx' dy', \quad (6)$$

which is the two-dimensional (2D) convolution of $U(x, y, 0)$ and transfer function of propagation $H(x, y, z)$, defined as

$$H(x, y, z) := \frac{e^{ikz}}{i\lambda z} e^{i\frac{\pi}{\lambda z}(x^2 + y^2)}. \quad (7)$$

The initial field was set to $U(x, y, 0) = U_0 \cdot P$, where U_0 is the beam profile (plane wave or wide Gaussian). A plane-wave description is sufficient to describe the experiment since the pinhole is much smaller than the Gaussian width of the beam and $P(x, y)$ represents the barrier function (aperture) defined by the first pinhole at $z = 0$,

$$P(x, y) = \begin{cases} 1, & \sqrt{x^2 + y^2} \leq R, \\ 0, & \sqrt{x^2 + y^2} > R, \end{cases} \quad (8)$$

where R is the pinhole radius. The resulting propagated field was split into real and imaginary components, a and b , and phase ϕ as in Eq. (1). The k -vector elements are calculated numerically from the phase gradient according to Eq. (2).

The experimental results and theoretical predictions are presented in Fig. 3. The red dotted line shows the theoretical prediction, which is made by considering the propagation of the angular spectrum of the light from the pinhole to the detection plane. The general linear trend of both the theoretical

and experimental curves shown is the expected trivial transverse displacement of the observed source when the camera is moving horizontally. This accounts for the relative lateral shift of the two pinholes as the small pinhole propagates. The linear behavior is interrupted by a series of sharp shifts at the interference minima where A is small. In these k -vector spikes, it would appear as if the source jumps to a new lateral position relative to the camera, such that the k vector becomes parallel to the optical axis. Thus, the image looks as though the source abruptly moved to a new position, as depicted in Fig. 1, which is the “optical ventriloquism” effect. These spikes also indicate clear deviations from the standard eikonal equation of ray optics. Additionally, it should be noted that the asymmetry of the shifts with respect to the central camera position is likely a result of imperfect alignment of the two pinholes relative to the optical axis.

V. CONCLUSION

In this paper, we experimentally demonstrated a phenomenon that we call “optical ventriloquism,” where light locally appears as if it came from a fictitious source that is located in a different place from the actual source. Revisiting the Helmholtz equation reveals that the ray-tracing equations of geometric optics must be corrected in regions where the wave amplitude rapidly changes. The local wave vector becomes superoscillatory, which causes light rays to bend locally and thus seem to come from a different direction. Notably, this self-bending of the rays is a consequence of wave interference and occurs independently of any local properties of the medium. A local observer who intercepts such a bent light ray would thus assume that standard ray-tracing methods apply and incorrectly infer the direction to the source.

As a proof of principle, we use the rapid amplitude changes near an interference fringe from the diffraction through a single-slit source to produce the ventriloquism effect. We

measure the direction of the local wave vector at different positions in the far field using a pair of pinholes placed before a camera. Our data in Fig. 3 show that the transverse local wave-vector component tends towards zero near any interference minima in the far field, regardless of the angle between that location and the source. Thus, at one of these locations the collected light appears to come from a direction orthogonal to the camera plane and not from the actual location of the source.

We anticipate that this ventriloquism effect can be controlled for specific applications by engineering the interference pattern produced from a more complex source. For example, a phased array of sources could be used to spoof or obscure the location of the array for observers who intercept the light only within a targeted spatial region. The limitations and specific applications of such a spoofing technique are topics for further investigation.

ACKNOWLEDGMENTS

This research was supported by the Fetzer-Franklin Fund of the John E. Fetzer Memorial Trust and by Grant No. FQXi-RFP-CPW-2006 from the Foundational Questions Institute and Fetzer Franklin Fund, a donor-advised fund of Silicon Valley Community Foundation. Y.A. thanks the Federico and Elvia Faggini Foundation for support. J.D. was supported by NSF-BSF Grant Award No. 1915015 and the Army Research Office (ARO) Grant No. W911NF-22-1-0258. E.C. was supported by the Israeli Innovation Authority under Project No. 73795, by the Pazy Foundation, by the Israeli Ministry of Science and Technology, and by the Quantum Science and Technology Program of the Israeli Council of Higher Education. J.C.H. acknowledges support from the Hebrew University and H2020-FETOPEN Grant No. 828946, and Chapman University.

-
- [1] Y. Aharonov, S. Popescu, and D. Rohrlich, How can an infra-red photon behave as a gamma ray? Tel-Aviv University Preprint TAUP 1847-90 (1990).
 - [2] M. V. Berry, *J. Phys. A: Math. Gen.* **27**, L391 (1994).
 - [3] M. V. Berry, *Faster than Fourier* (World Scientific, Singapore, 1994), pp. 55–65.
 - [4] M. V. Berry and S. Popescu, *J. Phys. A: Math. Gen.* **39**, 6965 (2006).
 - [5] M. R. Dennis, A. C. Hamilton, and J. Courtial, *Opt. Lett.* **33**, 2976 (2008).
 - [6] P. J. S. Ferreira and A. Kempf, *IEEE Trans. Signal Process.* **54**, 3732 (2006).
 - [7] E. Katzav and M. Schwartz, *IEEE Trans. Signal Process.* **61**, 3113 (2013).
 - [8] Y. Aharonov, F. Colombo, I. Sabadini, D. Struppa, and J. Tollaksen, *The Mathematics of Superoscillations* (American Mathematical Society, Providence, RI, 2017), Vol. 247.
 - [9] M. Berry, N. Zheludev, Y. Aharonov, F. Colombo, I. Sabadini, D. C. Struppa, J. Tollaksen, E. T. F. Rogers, F. Qin, M. Hong *et al.*, *J. Opt.* **21**, 053002 (2019).
 - [10] G. Chen, Z. Wen, and C. Qiu, *Light: Sci. Appl.* **8**, 56 (2019).
 - [11] S. Brehm, A. Akimov, R. Champion, and A. Kent, *Phys. Rev. Res.* **2**, 023009 (2020).
 - [12] Y. Shen, Y. Peng, F. Cai, K. Huang, D.-G. Zhao, C.-W. Qiu, H. Zheng, and X.-F. Zhu, *Nat. Commun.* **10**, 3411 (2019).
 - [13] A. M. Wong and G. Eleftheriades, *IEEE Microw. Wireless Compon. Lett.* **22**, 147 (2012).
 - [14] M. Berry and P. Shukla, *J. Phys. A: Math. Gen.* **45**, 015301 (2011).
 - [15] G. Yuan, S. Vezzoli, C. Altuzarra, E. TF Rogers, C. Couteau, C. Soci, and N. I. Zheludev, *Light: Sci. Appl.* **5**, e16127 (2016).
 - [16] Y. Aharonov, F. Colombo, I. Sabadini, D. Struppa, and J. Tollaksen, *J. Phys. A: Math. Gen.* **44**, 365304 (2011).
 - [17] Y. Aharonov, D. Z. Albert, and L. Vaidman, *Phys. Rev. Lett.* **60**, 1351 (1988).
 - [18] M. Berry and P. Shukla, *J. Phys. A: Math. Gen.* **43**, 354024 (2010).
 - [19] A. Hosoya and Y. Shikano, *J. Phys. A: Math. Gen.* **43**, 385307 (2010).
 - [20] M. F. Pusey, *Phys. Rev. Lett.* **113**, 200401 (2014).
 - [21] Y. Aharonov, E. Cohen, A. Carmi, and A. C. Elitzur, *Proc. R. Soc. A* **474**, 20180030 (2018).

- [22] M. R. Dennis and J. B. Götte, *New J. Phys.* **14**, 073013 (2012).
- [23] J. B. Götte and M. R. Dennis, *New J. Phys.* **14**, 073016 (2012).
- [24] M. R. Dennis and J. B. Götte, *Phys. Rev. Lett.* **109**, 183903 (2012).
- [25] M. R. Dennis and J. B. Götte, *J. Opt.* **15**, 014015 (2013).
- [26] J. B. Götte and M. R. Dennis, *Opt. Lett.* **38**, 2295 (2013).
- [27] M. V. Berry, *Light: Sci. Appl.* **12**, 238 (2023).
- [28] M. V. Berry and M. Dennis, *J. Phys. A: Math. Gen.* **42**, 022003 (2008).
- [29] M. V. Berry, *J. Opt. A: Pure Appl. Opt.* **11**, 094001 (2009).
- [30] S. Kocsis, B. Braverman, S. Ravets, M. J. Stevens, R. P. Mirin, L. K. Shalm, and A. M. Steinberg, *Science* **332**, 1170 (2011).
- [31] K. Y. Bliokh, A. Y. Bekshaev, A. G. Kofman, and F. Nori, *New J. Phys.* **15**, 073022 (2013).
- [32] M. V. Berry, *Eur. J. Phys.* **42**, 015401 (2020).
- [33] J. W. Goodman, *Introduction to Fourier Optics*, 3rd ed. (Roberts & Company, Englewood, CO, 2005), Vol. 1.
- [34] D. A. Steck, *Classical and Modern Optics*, available online at <http://steck.us/teaching> (2006).
- [35] Video available at https://drive.google.com/file/d/1Na7gc9uP5B-UbCAb_hXIZPOdaN_oIQau/view?usp=sharing.